RESEARCH PAPER

Synthesis and Antibacterial with Characterization Activity of Poly (Ethylene Oxide)/Tungsten Dioxide Nanocomposites

Mays Sabah Mahdi [1], Farah H. Rashid [1], Riyam Edan Hawy [1], Noor M alik Saadoon [2]

[1] Collage of Biomedical Instrumentation Engineering, University of Technology, Iraq

[2] Institute of Nanotechnology and Advanced Materials Research for Postgraduate Studies, University of Technology, Iraq

ARTICLE INFO

Article History:
Received 13 March 2026
Accepted 25 June 2026
Published 01 July 2026

Keywords:
Antibacterial activity
Escherichia coli
Nanocomposite
Spin coating
Tungsten dioxide
UV–Visible spectroscopy

ABSTRACT

In this study, Poly(ethylene oxide) (PEO)/Tungsten Dioxide (WO_2) nanocomposite thin films containing 30 wt.% WO_2 nanoparticles were successfully prepared using the spin-coating technique. The structural, chemical, and optical properties of the prepared nanocomposites were investigated using X-ray diffraction (XRD), Fourier-transform infrared spectroscopy (FTIR), and UV–Visible spectroscopy. XRD analysis revealed that the incorporation of WO_2 nanoparticles modified the crystalline structure of the PEO matrix, indicating effective interaction between the polymer chains and the Nanomaterial. FTIR spectra confirmed the presence of characteristic functional groups and suggested intermolecular interactions between PEO and WO_2 without the formation of undesirable chemical species. UV–Visible measurements demonstrated enhanced optical absorption and reduced transmittance after the addition of WO_2, reflecting the influence of the nanoparticles on the optical behavior of the nanocomposite. The antibacterial activity was evaluated against Escherichia coli using the agar well diffusion method. The prepared nanocomposite exhibited concentration-dependent antibacterial activity, with the largest inhibition zone observed at the highest concentration, demonstrating improved antibacterial performance. These findings indicate that Poly (ethylene oxide)/Tungsten Dioxide nanocomposites possess promising structural, optical, and antibacterial properties, making them suitable candidates for future biomedical and antimicrobial applications.

How to cite this article
Mahdi M., H. Rashid F., Hawy R., Saadoon N. Synthesis and Antibacterial with Characterization Activity of Poly (Ethylene Oxide)/Tungsten Dioxide Nanocomposites . J Nanostruct, 2026; 16(3):4075-4084. DOI: 10.22052/JNS.2026.03.091

INTRODUCTION

The rapid emergence of antibiotic-resistant bacteria has become one of the most significant challenges to global public health, limiting the effectiveness of conventional antimicrobial therapies and increasing the demand for the development of alternative antibacterial materials. In recent years, nanotechnology has provided new opportunities for designing advanced materials with enhanced biological performance [1]. In particular, polymer-based nanocomposites have attracted considerable attention because they combine the advantageous properties of polymer matrices with the unique physicochemical characteristics of nanomaterials, leading to multifunctional systems with improved structural, optical, mechanical, and biological properties [2].

The incorporation of nanoparticles into

* Corresponding Author Email: mae.visit.04@uotechnology.edu.iq

polymer matrices has become an effective strategy for tailoring the performance of polymeric materials without compromising their flexibility or processability. Owing to their high surface-to-volume ratio and unique interfacial interactions, nanoparticles can significantly modify the crystallinity, morphology, thermal stability, optical behavior, and surface properties of polymers [3]. Consequently, polymer nanocomposites have been widely investigated for numerous applications, including biomedical engineering, drug delivery, tissue engineering, biosensors, wound dressings, food packaging, environmental remediation, and antibacterial materials [4]. Among synthetic polymers, poly(ethylene oxide) (PEO) has received considerable attention because of its excellent biocompatibility, non-toxicity, flexibility, and ease of processing. In addition, its semi-crystalline structure and compatibility with a wide range of inorganic nanomaterials make it an attractive polymer matrix for the fabrication of functional nanocomposites. Despite these advantages, pure PEO exhibits limited intrinsic antibacterial activity, which restricts its direct application in environments requiring efficient microbial inhibition [5-7]. Therefore, the incorporation of functional nanomaterials into the PEO matrix has emerged as an effective approach to enhance its physicochemical and biological performance.

Transition metal oxides are among the most extensively investigated nanomaterials because of their chemical stability, structural diversity, and functional properties. Tungsten oxides, in particular, have attracted increasing research interest owing to their optical, electrical, and surface characteristics, as well as their compatibility with polymeric matrices. Tungsten dioxide (WO_2) is a metallic oxide phase with distinctive structural and electronic properties that make it a promising candidate for incorporation into polymer-based nanocomposites [8]. The addition of WO_2 nanoparticles is expected to influence the structural organization, surface morphology, and optical behavior of the polymer matrix, which may consequently affect its antibacterial performance.

The antibacterial behavior of polymer/metal oxide nanocomposites is generally associated with the interaction between nanoparticle surfaces and bacterial cells. These interactions can alter bacterial membrane integrity, interfere with essential cellular functions, and inhibit bacterial proliferation. The efficiency of these processes is influenced by several factors, including nanoparticle size, dispersion within the polymer matrix, surface characteristics, and the interfacial interaction between the polymer and the nanomaterial [9]. Therefore, investigating the relationship between the structural properties of PEO/WO_2 nanocomposites and their antibacterial activity is essential for the development of advanced antibacterial materials [10].

Although polymer/metal oxide nanocomposites have been extensively studied, investigations specifically focusing on PEO/WO_2 nanocomposites for antibacterial applications remain limited. Accordingly, the present study aims to synthesize a PEO/WO_2 nanocomposite and investigate its structural, morphological, and optical properties using X-ray diffraction (XRD), scanning electron microscopy (SEM), and UV–Visible spectroscopy. Furthermore, the antibacterial activity of the prepared nanocomposite is evaluated against representative bacterial strains to assess its potential as an antibacterial material for future biomedical applications.

MATERIALS AND METHODS

Preparation of Poly(ethylene oxide)/Tungsten Dioxide Nanocomposite Thin Films

Poly(ethylene oxide) powder was dissolved in 25 mL of Dimethylformamide under continuous magnetic stirring at 60 °C for approximately 1 h until a homogeneous solution was obtained. Tungsten dioxide nanoparticles, corresponding to 30 wt. % of the polymer weight, were separately dispersed in 20 mL of DMF under continuous stirring and then gradually added to the PEO solution. The resulting mixture was continuously stirred at 65 °C for 4 h to ensure homogeneous dispersion of the nanoparticles within the polymer matrix. The prepared nanocomposite solution was deposited onto clean glass substrates using the spin-coating technique. The coating process was carried out in three successive stages and the obtained films were allowed to dry completely, resulting in uniform Poly(ethylene oxide)/Tungsten Dioxide nanocomposite thin films, which were subsequently used for structural, morphological, optical, and antibacterial characterization.

RESULTS AND DISCUSSION

The X-ray diffraction (XRD) pattern of pure PEO

The X-ray diffraction (XRD) pattern of pure PEO exhibits a characteristic semi-crystalline structure, with a prominent diffraction peak centered at 2θ = 23.25°, indicating the presence of ordered crystalline domains formed by the regular arrangement of polyethylene oxide chains. In addition to the main diffraction peak, the broad background observed in the diffractogram reflects the coexistence of amorphous regions, which is a typical structural feature of PEO. The coexistence of crystalline and amorphous phases confirms the semi-crystalline nature of the polymer, while the absence of additional diffraction peaks suggests that no detectable crystalline impurities are present in the sample [11]. As seen in Fig. 1.

The X-ray diffraction patterns of pure Poly(ethylene oxide) and the Poly(ethylene oxide)/30 wt.%Tungsten Dioxide nanocomposite Fig. 2, reveal a clear modification in the crystalline structure following the incorporation of WO_2 nanoparticles. Pure PEO exhibits a characteristic diffraction peak at 2θ = 23.25°, confirming its

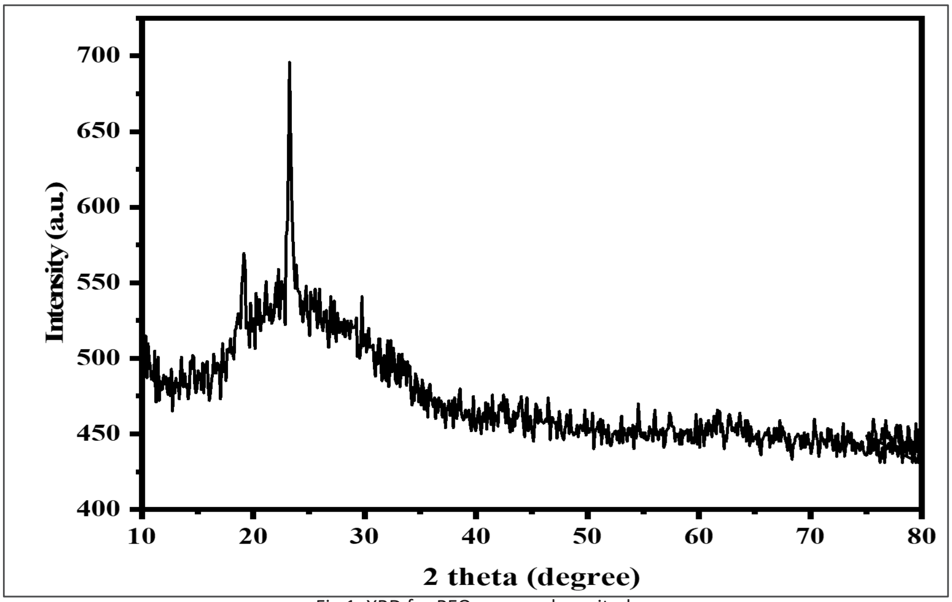

Fig 1. XRD for PEO pure as deposited.

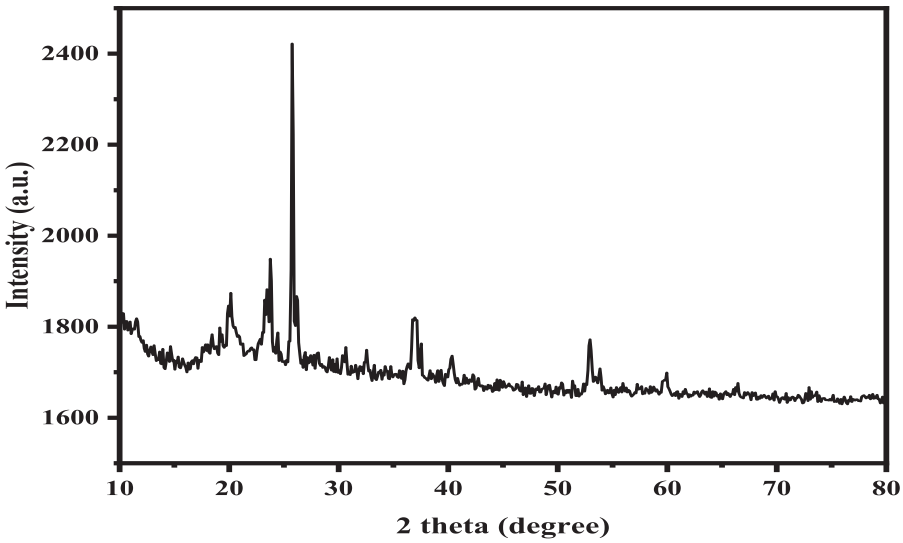

Fig 2. XRD for PEO doping with WO2 nanocomposite thin film.

semi-crystalline nature. After the addition of 30 wt.% WO_2, the main diffraction peak shifts to 2θ = 25.75°, accompanied by a substantial increase in diffraction intensity from approximately 696 to 2422 a.u. This enhancement in intensity indicates an increase in the overall crystallinity of the nanocomposite, which can be attributed to the crystalline contribution of WO_2 nanoparticles and

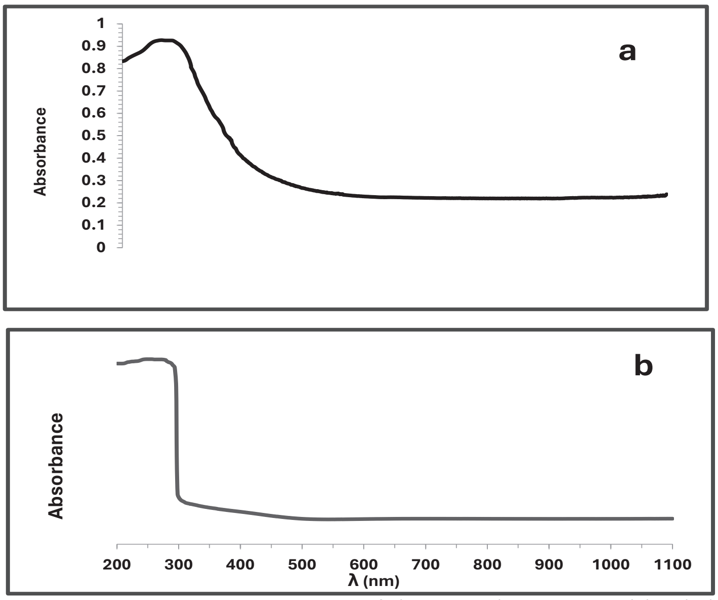

Fig 3. The UV–Visible absorption spectra of a) pure Poly(ethylene oxide) (PEO) b) Poly(ethylene oxide)/Tungsten Dioxide (WO_2) nanocomposite.

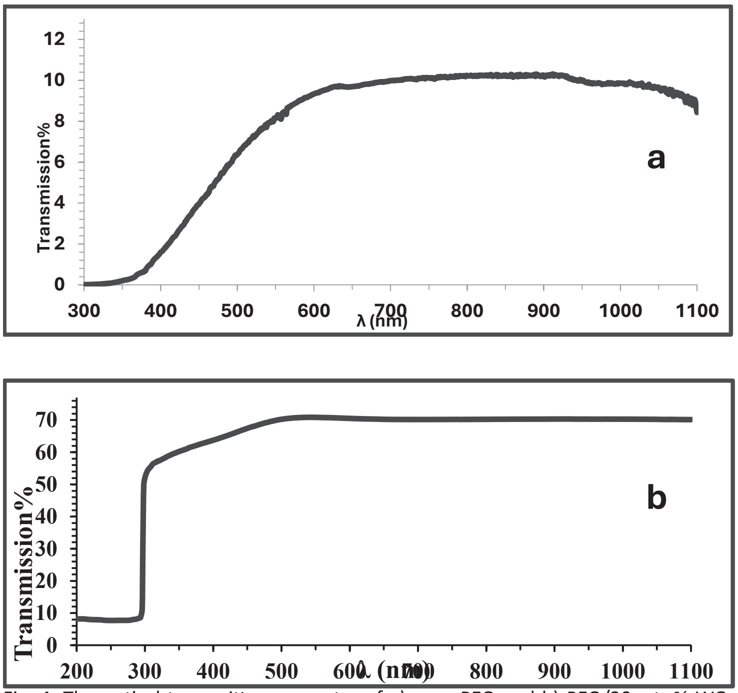

Fig. 4. The optical transmittance spectra of a) pure PEO and b) PEO/30 wt. % WO_2 nanocomposite.

their interaction with the PEO matrix. The shift in the diffraction peak suggests that the incorporation of WO_2 affects the molecular packing of the polymer chains, leading to structural rearrangement within the composite. These observations confirm the successful incorporation of tungsten dioxide nanoparticles into the PEO matrix and demonstrate that the addition of WO_2 significantly influences the crystalline characteristics of the prepared nanocomposite [12].

UV–Visible Absorption Spectra

The UV–Visible absorption spectra of pure Poly(ethylene oxide) (PEO) and the Poly(ethylene oxide)/Tungsten Dioxide (WO_2) nanocomposite are presented in Fig. 3a and Fig. 3b, respectively. Pure PEO exhibits relatively low absorbance throughout the visible region, while a noticeable increase in absorbance is observed in the ultraviolet region. This behavior is characteristic of PEO due to its wide optical band gap and limited electronic transitions within the visible range. After the incorporation of 30 wt.% WO_2 nanoparticles, the absorbance of the nanocomposite increases over a broad wavelength range. This enhancement can be attributed to the strong interaction between the incident photons and WO_2 nanoparticles, which introduce additional electronic states and improve light absorption. The increased absorbance confirms the successful incorporation of WO_2 into the polymer matrix and indicates a significant modification of the optical properties of the prepared nanocomposite [13].

Optical Transmittance pure PEO and doping nanocomposite

The optical transmittance spectra of pure PEO and the PEO/30wt.% WO_2 nanocomposite are shown in Fig. 4a and Fig. 4b. Pure PEO exhibits high optical transparency over most of the visible spectral region owing to its relatively low absorption coefficient. Following the incorporation of WO_2 nanoparticles, the transmittance decreases considerably, particularly in the ultraviolet region. This reduction in transmittance is associated with the increased absorption and scattering of incident light by the dispersed WO_2 nanoparticles. The decrease in optical transparency confirms the interaction between the polymer matrix and the inorganic nanoparticles and further demonstrates the influence of WO_2 on the optical behavior of the prepared nanocomposite [14].

The optical band gap of the prepared Poly(ethylene oxide)/Tungsten Dioxide nanocomposite was determined using the Tauc relation by plotting $(\alpha h\nu)^2$ versus photon energy ($h\nu$), as illustrated in Fig. 5. The optical band gap was obtained by extrapolating the linear portion of the curve to the energy axis. The incorporation of WO_2 nanoparticles modifies the electronic structure of the polymer matrix by introducing localized energy states within the forbidden band, thereby affecting the optical transition process. Such behavior is commonly observed in polymer nanocomposites containing transition metal oxide nanoparticles and reflects the strong interaction between the polymer chains and the dispersed

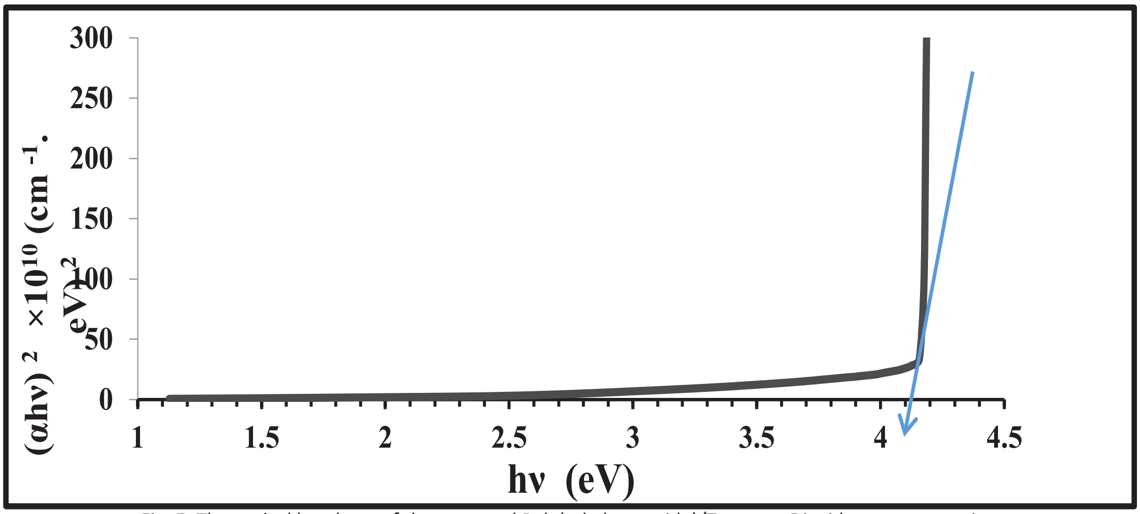

Fig. 5. The optical band gap of the prepared Poly(ethylene oxide)/Tungsten Dioxide nanocomposite.

nanocomposite [15].

Fourier Transform Infrared (FTIR) Analysis

The FTIR spectra of pure Poly(ethylene oxide) (PEO) and the Poly(ethylene oxide)/30 wt.% Tungsten Dioxide (WO_2) nanocomposite are presented in Fig. 6, respectively. The spectrum of pure PEO exhibits the characteristic absorption bands associated with the polymer backbone, confirming the chemical structure of polyethylene oxide. After the incorporation of WO_2 nanoparticles, noticeable variations in the intensity and position of several absorption bands are observed. These changes indicate the interaction between the polymer chains and the dispersed WO_2 nanoparticles, suggesting the formation of interfacial interactions within the nanocomposite. No additional absorption bands corresponding to undesirable chemical species are detected, indicating that the preparation process did not introduce new chemical impurities. The observed spectral changes support the successful incorporation of WO_2 nanoparticles into the PEO matrix and are consistent with the structural modifications observed in the XRD analysis [16].

Prepare of Mueller Hinton agar

Muller-Hinton (M-H) prepared by adding 38 g of the powder into 1 L distilled water

then heated on a burner with shaking. M-H must be autoclaved for 15 minutes at 121°C to be sterilized. Then it was allowed to cool to 50 °C before pouring into a petri dish and leaving for about 15 minutes for solidification before flipping upside down and storing in the refrigerator at 4 °C.

Antibacterial activity

The antibacterial potential of the prepared nanocomposites was investigated against Gram's negative and Gram's positive bacterial strains using agar well diffusion assay [17, 18]. About 20mL of on Muller–Hinton (MH) agar was aseptically poured into sterile Petri dishes. The bacterial species were collected from their stock cultures using a sterile wire loop [3]. After culturing the organisms, 6 mm-diameter wells were bored on the agar plates using of a sterile tip. Into the bored wells, different concentrations of the Sample were used. The cultured plates containing the Sample and the test organisms were incubated overnight at 37°C [19,20].

Antibacterial Activity of the prepared Poly(ethylene oxide)/Tungsten Dioxide nanocomposite

The antibacterial activity of the prepared Poly(ethylene oxide)/Tungsten Dioxide nanocomposite was evaluated using the agar well diffusion method, as shown in Fig. 7. The results demonstrate the formation of clear inhibition zones around the wells containing the tested samples, confirming the antibacterial activity of the prepared nanocomposite against the investigated bacterial strain [21]. However, the inhibition zones varied among the tested samples, indicating differences in antibacterial effectiveness. Samples C, D, and E exhibited relatively larger inhibition zones than samples A and B, suggesting stronger antibacterial activity. The enhanced antibacterial

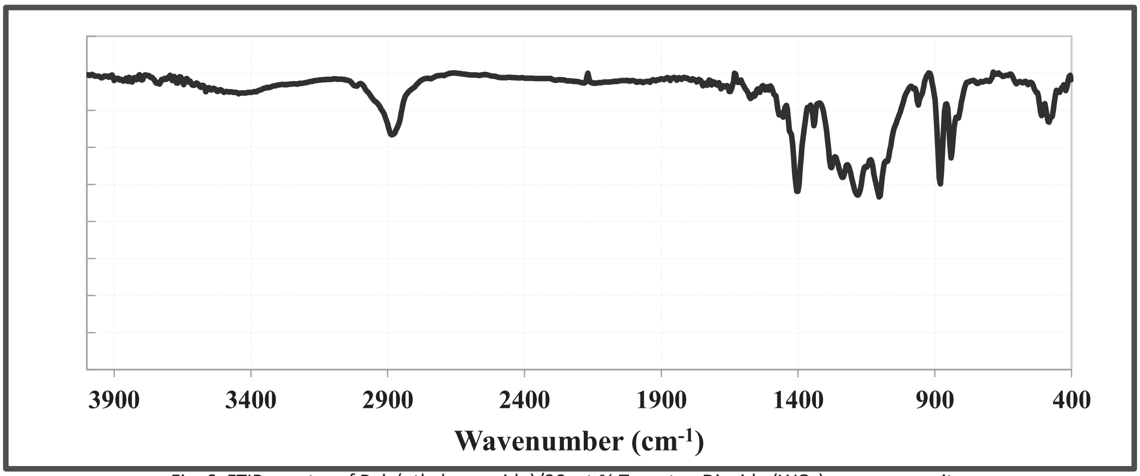

Fig. 6. FTIR spectra of Poly(ethylene oxide)/30 wt.% Tungsten Dioxide (WO_2) nanocomposite.

performance can be attributed to the presence of tungsten dioxide nanoparticles, which increase the interaction between the nanocomposite surface and bacterial cells, thereby suppressing bacterial growth. The antibacterial behavior is also consistent with the structural modifications observed in the XRD analysis and the changes in the optical properties revealed by UV–Visible spectroscopy, confirming that the incorporation of WO_2 nanoparticles significantly improves the

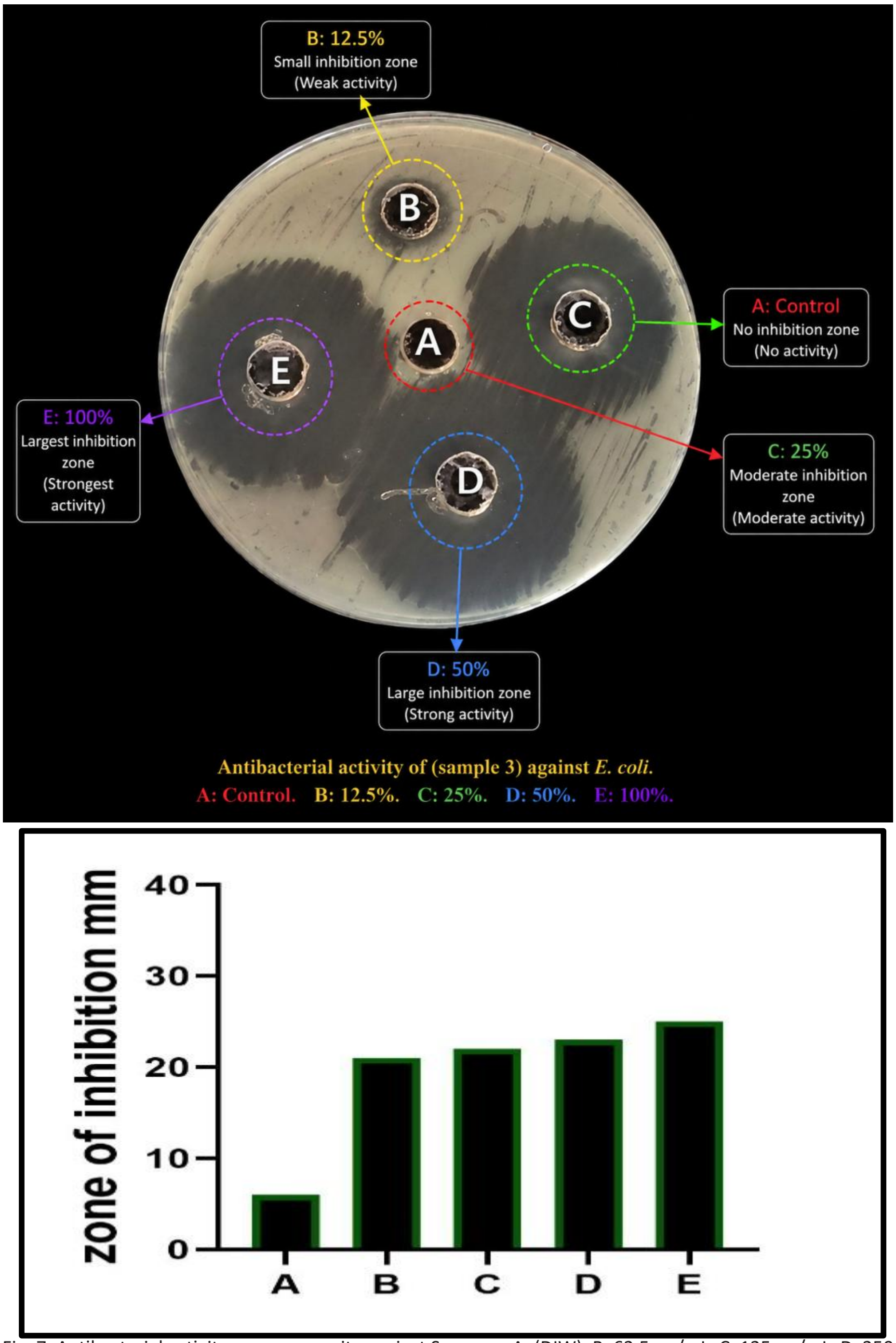

Fig. 7. Antibacterial activity nanocomposite against S.aureus. A, (DIW). B, 62.5 µg/mL. C, 125 µg/mL. D, 250 µg/mL. E, 500 µg/mL.

functional performance of the Poly(ethylene oxide) matrix [22-23].

The antibacterial activity of the prepared Poly(ethylene oxide)/Tungsten Dioxide (PEO/WO_2) nanocomposite was evaluated against Escherichia coli using the agar well diffusion method, as shown in Fig. 8. The control sample (A) exhibited no inhibition zone, confirming the absence of antibacterial activity in the control. In contrast, all tested concentrations of the PEO/WO_2 nanocomposite (12.5%, 25%, 50%, and 100%) produced visible inhibition zones around the wells, indicating effective antibacterial activity against E. coli. Furthermore, the inhibition zone gradually increased with increasing nanocomposite concentration. The 12.5% concentration (B) showed the smallest inhibition zone, whereas the 25% (C) and 50%

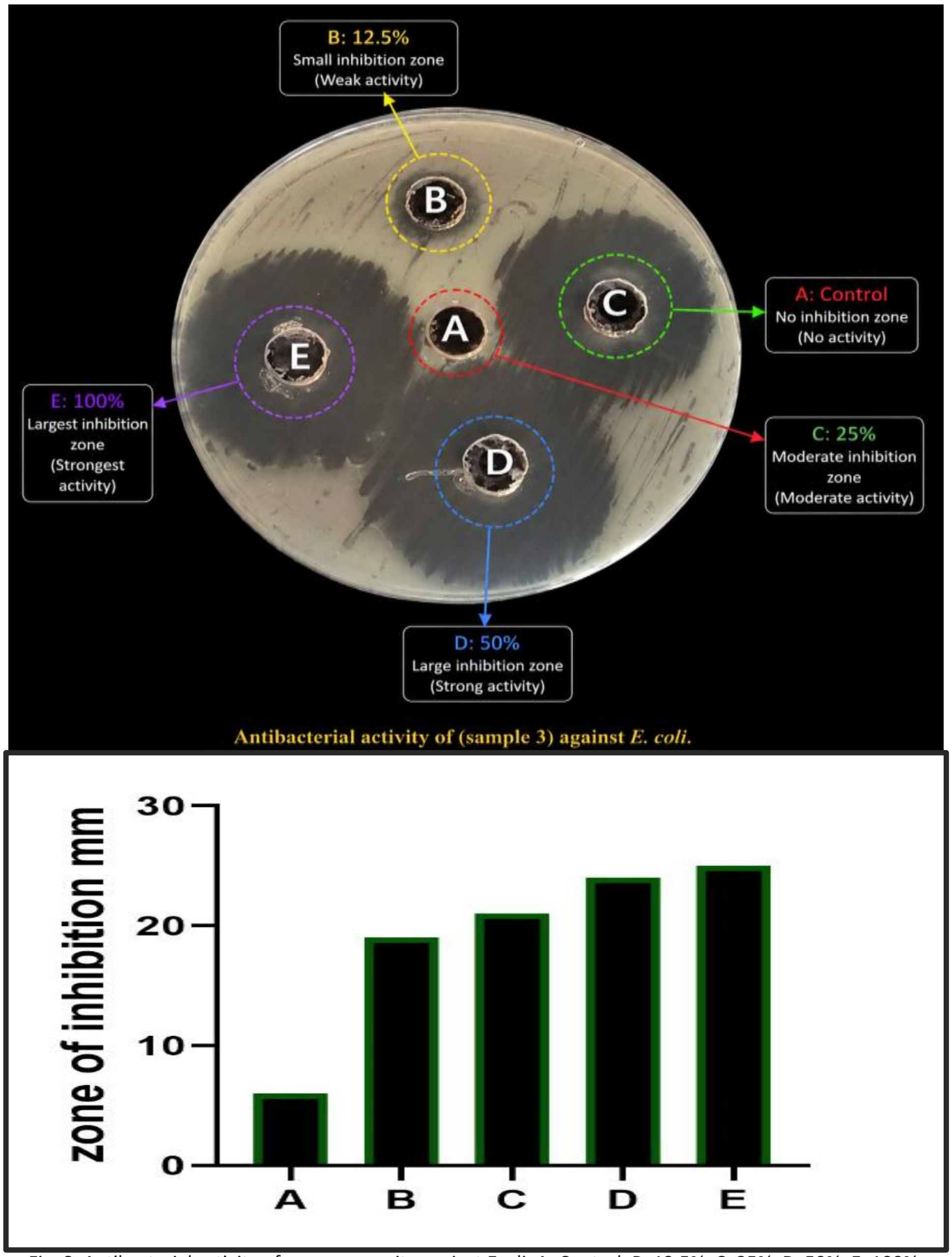

Fig. 8. Antibacterial activity of nanocomposite against Ecoli. A, Control. B, 12.5%. C, 25%. D, 50%. E, 100%.

(D) concentrations exhibited progressively larger inhibition zones. The largest inhibition zone was observed at the 100% concentration (E), demonstrating the highest antibacterial efficiency. This concentration-dependent antibacterial behavior suggests that increasing the amount of the PEO/WO_2 nanocomposite enhances its ability to suppress bacterial growth. The improved antibacterial performance can be attributed to the presence of WO_2 nanoparticles, which increase the interaction with bacterial cells and may induce oxidative stress and membrane damage, ultimately inhibiting bacterial proliferation. These findings demonstrate that the prepared PEO/WO_2 nanocomposite possesses promising antibacterial properties and may be considered a potential material for antibacterial coating and biomedical applications [24].

CONCLUSION

Poly (ethylene oxide)/Tungsten Dioxide (PEO/WO_2) nanocomposite thin films were successfully prepared using the spin-coating technique. The incorporation of 30 wt.% WO_2 nanoparticles effectively modified the structural and optical properties of the PEO matrix, as confirmed by X-ray diffraction (XRD), Fourier-transform infrared (FTIR), and UV–Visible spectroscopy analyses. The XRD results indicated changes in the crystalline structure of the polymer after the addition of WO_2, while FTIR analysis suggested intermolecular interactions between the polymer matrix and the nanoparticles without the formation of undesirable chemical species. UV–Visible measurements demonstrated enhanced optical absorption accompanied by reduced transmittance, confirming the influence of WO_2 nanoparticles on the optical behavior of the nanocomposite. Furthermore, the antibacterial evaluation against Escherichia coli revealed concentration-dependent antibacterial activity, with the highest concentration exhibiting the greatest inhibition of bacterial growth. Overall, the prepared PEO/WO_2 nanocomposite exhibits promising structural, optical, and antibacterial characteristics were indicating its potential for use in antibacterial coatings and other biomedical applications.

CONFLICT OF INTEREST

The authors declare that there is no conflict of interests regarding the publication of this manuscript.

REFERENCES

1. Salman ON, Ahmed DS, Abed AL, Dawood MO. Preparation pure ZnO, La-doped ZnO nanoparticles using sol-gel technique: Characterization and Evaluation Antibacterial Activity. IOP Conference Series: Materials Science and Engineering. 2019;518(3):032012.
2. Staudinger U, Janke A, Simon F, Jakisch L, Bittrich E, Formanek P, et al. MWCNT Localization and Electrical Percolation in Thin Films of Semifluorinated PMMA Block Copolymers. Polymers. 2025;17(9):1271.
3. Samadi A, Haseli S, Pourmadadi M, Rashedi H, Yazdian F, Navaei-Nigjeh M. Curcumin-loaded Chitosan-Agarose-Montmorillonite Hydrogel Nanocomposite for the Treatment of Breast Cancer. 2020 27th National and 5th International Iranian Conference on Biomedical Engineering (ICBME); 2020/11/26: IEEE; 2020. p. 148-153.
4. Mirzaie Z, Barati M, Tokmedash MA. Anticancer Drug Delivery Systems Based on Curcumin Nanostructures: A Review. Pharm Chem J. 2020;54(4):353-360.
5. The Influence of ZnO NPs on Reproductive System Tissues of Albino Male Mice. Histopathological Study. International Journal of Science and Research (IJSR). 2017;6(7):2021-2025.
6. Saadoon AM, Hmoad NR, Hussein SG, Abdullah MQ. Finite-element guided drilled-hole placement and fillet geometry effects on the structural and dynamic performance of spur gears. Frontiers in Mechanical Engineering. 2026;12.
7. Synthesis and Characterization of Tetrahydropyran-Based Bacterial Topoisomerase Inhibitors with Antibacterial Activity against Gram-Negative Bacteria. American Chemical Society (ACS).
8. Shabnam H, Mehrab P, Amirmasoud S, Fatemeh Y, Majid A, Hamid R, et al. Author response for "A novel pH-responsive nanoniosomal emulsion for sustained release of curcumin from a chitosan-based nanocarrier: emphasis on the concurrent improvement of loading, sustained release, and apoptosis induction". Wiley; 2022.
9. Jasim AJ, Yusop MR, Taha BA, Al-Amiery AA, Saadoon NM, Akhtar MF, et al. Sustainable development of novel zinc oxide nano flowers mediated red yeast rice for control of hepatocellular carcinoma. Sci Rep. 2026;16(1).
10. Gharawi MA, Saadoon AM, Hmoad NR, Albayati AH. Structural performance of rail connections: Experimental testing and finite element modeling. Results in Engineering. 2025;27:105997.
11. Lee ALZ, Wang Y, Cheng HY, Pervaiz S, Yang YY. The co-delivery of paclitaxel and Herceptin using cationic micellar nanoparticles. Biomaterials. 2009;30(5):919-927.
12. Sun C, Lee JSH, Zhang M. Magnetic nanoparticles in MR imaging and drug delivery. Adv Drug Del Rev. 2008;60(11):1252-1265.
13. Mohammed MQ, Shugran AHM. Inhibitory effect of silver oxide nanoparticles and Saccharomyces cerevisiae on Escherichia coli and Staphylococcus aureus bacteria. Experimental and Theoretical NANOTECHNOLOGY. 2026;10(1):13-23.
14. Yu MK, Park J, Jon S. Targeting Strategies for Multifunctional Nanoparticles in Cancer Imaging and Therapy. Theranostics. 2012;2(1):3-44.
15. Kadhim AA-A, Ali AA-R, Sura AS. Improved Stress State Calculation for Geosynthetic-Encased Columns Using

Granular Media Mechanics. Archives for Technical Sciences. 2026.
16. Alshathr AH, Hatem T, Al-Majeed MA, Saadoon NM, Rahmah MI. Breakdown Spectroscopy Stimulate by Laser for Silver Plasma. Neuroquantology. 2022;20(1):84-89.
17. Davarpanah AM, Rahdar A, Dastnae MA, Zeybek O, Beyzaei H. (1-x)$BaFe_{12}O_{19}$/ $xCoFe_2O_4$ hard/soft magnetic nanocomposites: Synthesis, physical characterization, and antibacterial activities study. J Mol Struct. 2019;1175:445-449.
18. Saadoon AM, Al Gharawi M, Al-Mosawe A. Effect of Elevated Temperature on Microstructure and Mechanical Properties of Hot-Rolled Steel. Engineering, Technology and Applied Science Research. 2024;14(6):18756-18766.
19. Qiao Z, Shi X. Dendrimer-based molecular imaging contrast agents. Prog Polym Sci. 2015;44:1-27.
20. Rahdar A, Taboada P, Aliahmad M, Hajinezhad MR, Sadeghfar F. Iron oxide nanoparticles: Synthesis, physical characterization, and intraperitoneal biochemical studies in Rattus norvegicus. J Mol Struct. 2018;1173:240-245.
21. Ahmadi M, Pourmadadi M, Ghorbanian SA, Yazdian F, Rashedi H. Ultra pH-sensitive nanocarrier based on Fe2O3/chitosan/montmorillonite for quercetin delivery. Int J Biol Macromol. 2021;191:738-745.
22. Abdalsalam AH, Saadoon NM, Ati AA, Dabagh S, Salim A. Investigation of the structural, morphological, and electrochemical characteristics of $MgFe_2O_4$/ZnO nanocomposite. Al-Qadisiyah Journal for Engineering Sciences. 2025;18(4):352-359.
23. Hmoad NR, Ali AH, Saadoon AM, Abdulkareem AA, Albayati AH. Effect of different wing geometries on their vibration characteristics. Frontiers in Mechanical Engineering. 2026;11.
24. Jasim Yousif H, Ameer A, Kareem Sulaiman H. Cutoff fuzzy dominating set of strong fuzzy graph. Journal of Discrete Mathematical Sciences and Cryptography. 2025;28(2):577-585.